Hypomorphic Rag mutations can cause destructive midline granulomatous disease

Suk See De Ravin,[1] Edward W. Cowen,[2] Kol A. Zarember,[1] Narda L. Whiting-Theobald,[1] Douglas B. Kuhns,[3] Netanya G. Sandler,[4] Daniel C. Douek,[4] Stefania Pittaluga,[5] Pietro L. Poliani,[6] Yu Nee Lee,[7] Luigi D. Notarangelo,[7] Lei Wang,[7] Frederick W. Alt,[7] Elizabeth M. Kang,[1] Joshua D. Milner,[1] Julie E. Niemela,[8] Mary Fontana-Penn,[9] Sara H. Sinal,[9] and Harry L. Malech[1]

[1]Laboratory of Host Defenses, National Institute of Allergy and Infectious Diseases and [2]Dermatology Branch, National Cancer Institute, National Institutes of Health (NIH), Bethesda, MD; [3]Clinical Services Program, SAIC-Frederick Inc, Frederick, MD; [4]Vaccine Research Center, [5]Pathology, National Cancer Institute, NIH, Bethesda, MD; [6]Department of Pathology, University of Brescia, Brescia, Italy; [7]Division of Immunology, Children's Hospital Boston, Harvard Medical School, Boston, MA; [8]Department of Laboratory Medicine, Clinical Center, NIH, Bethesda, MD; [9]Department of Pediatrics, Wake Forest University School of Medicine, Winston-Salem, NC

Destructive midline granulomatous disease characterized by necrotizing granulomas of the head and neck is most commonly caused by Wegener granulomatosis, natural killer/T-cell lymphomas, cocaine abuse, or infections. An adolescent patient with myasthenia gravis treated with thymectomy subsequently developed extensive granulomatous destruction of midface structures, palate, nasal septum, airways, and epiglottis. His lymphocyte numbers, total immunoglobulin G level, and T-cell receptor (TCR) repertoire appeared normal. Sequencing of Recombination activating gene-1 (*Rag1*) showed compound heterozygous Rag1 mutations; a novel deletion with no recombinase activity and a missense mutation resulting in 50% Rag activity. His thymus was dysplastic and, although not depleted of T cells, showed a notable absence of autoimmune regulator (AIRE) and Foxp3$^+$ regulatory T cells. This distinct Rag-deficient phenotype characterized by immune dysregulation with granulomatous hyperinflammation and autoimmunity, with relatively normal T and B lymphocyte numbers and a diverse TCR repertoire expands the spectrum of presentation in Rag deficiency. This study was registered at www.clinicaltrials.gov as #NCT00128973. (*Blood*. 2010;116(8):1263-1271)

Introduction

Progressive granulomatous tissue destruction of the midface and the upper airways is most commonly caused by Wegener granulomatosis (WG) or malignancies such as natural killer (NK)/T-cell lymphomas and, to a lesser extent, cocaine abuse or infections.[1,2] The hallmark pathologic finding of destructive midline granulomatous (DMG) disease is caseating granulomas characteristically involving the nose, sinuses, palate, and upper airways, especially the subglottis. Although WG usually includes renal involvement and circulating antineutrophil antibodies (ANCAs), local nasopharyngeal WG without associated antibodies occurs.[3] Standard therapy for these diseases involves immunoablative chemotherapy to halt disease progression, in contrast to immunosupportive measures required to treat primary immune deficiencies. We describe in this report the first patient with clinical manifestations of a WG-like destructive midline granulomatosis with underlying novel compound heterozygote mutations in Rag1.

The recombination activation genes, *Rag1* and *Rag2*, perform a critical role in the somatic rearrangement and assembly of the modular genes for variable (V), diversity (D), and joining (J) gene segments of immunoglobulins and of antigen receptor genes.[4-6] After binding to conserved recombination signal sequences (RSSs) that flank individual V, D, or J gene segments, the Rag1/2 complex introduces a nick in the DNA, followed by formation of a coding end hairpin. Nonhomologous end joining DNA repair then takes place to generate the diverse VDJ contiguous regions that are essential for defense against many different pathogens. In addition to initiating the double-strand DNA breaks, the Rag complex stabilizes recombination intermediates to promote repair and editing of the modified genes.[6,7] Rag proteins are indispensable for lymphocyte development and differentiation, and defects in Rag manifests as T- and B-deficient severe combined immunodeficiency (T-B-SCID) or Omenn syndrome (OS) in infancy. These syndromes are characterized by early-onset profound deficiency in T and B cells for SCID and by early-onset erythroderma, hepatosplenomegaly, eosinophilia, and hyper immunoglobulin E (IgE) in OS.

In stark contrast, our patient presented for evaluation of a DMG process at 14 years of age with normal numbers of CD3$^+$ T and CD19$^+$/CD20$^+$ B cells and with normal total IgG levels. Evaluation in subsequent years showed dysregulated hyperinflammatory responses with appearance of new granulomatous lesions after environmental or viral triggers. This report further extends the clinical spectrum of *Rag* mutations, and our data support the view that, in addition to susceptibility to infections and autoimmunity, hyperinflammation is an important component of Rag deficiency and may be the primary clinical manifestation leading to diagnosis when lymphocyte counts are normal. Hypomorphic Rag mutations should be considered in "idiopathic" destructive granulomatous disease.

Methods

The subjects were enrolled on protocol 05-I-213 approved by the National Institute of Allergy and Infectious Diseases institutional review board. All

Submitted February 3, 2010; accepted April 17, 2010. Prepublished online as *Blood* First Edition paper, May 20, 2010; DOI 10.1182/blood-2010-02-267583.

investigations were conducted and informed consent obtained from all subjects in accordance with the Declaration of Helsinki.

Flow cytometric analysis

Peripheral blood was stained on ice with fluorochrome-conjugated monoclonal antibodies for 30 minutes, then erythrocytes were lysed by treatment with BD fluorescence-activated cell sorting (FACS) Lysing Solution (Becton Dickinson) for 10 minutes.[8] Monoclonal antibodies used include anti-CD3, -CD4, -CD8, CD16, -CD19, –T-cell receptor α/β (TCRα/β), -TCRγ/δ (Becton Dickinson) and human leukocyte antigen–A, –B, –C (BD PharMingen). Foxp3 monoclonal antibody was used per manufacturer's instructions (eBioscience). Analysis of the TCR Vβ repertoire of the lymphocytes by FACS (TCR Vβ Repertoire Kit; Beckman Coulter) was also performed with cells costained for CD4-allophycocyanin and CD8–phycoerythrin-cyanine 5 (BD PharMingen).

Vβ immunoscope (spectratype)

CDR3 size spectratyping was performed to analyze the TCR repertoire as previously described.[9] Briefly, RNA was extracted from peripheral blood mononuclear cell (PBMC) samples (1-5 × 10^6 cells/sample) with the use of STAT60 (Teletest) and reverse transcribed to cDNA with Superscript III (Invitrogen), which served as a template for 24 polymerase chain reactions (PCRs) with the use of previously described primers for the CDR3 region.[10] The amplified products were analyzed by capillary electrophoresis and GeneScan software (Applied Biosystems Inc). For sequencing, the PCR-amplified products were ligated to cloning vector (TOPO TA Cloning for Sequencing Kit). DNA isolated from colonies were amplified with the respective forward or reverse primers for the Vβ family (CEQ Terminator Cycle Sequencing Quick Start Kit; Beckman Coulter), and the products were analyzed on the CEQ8000 sequencer (Beckman Coulter).

Immunohistochemical analyses

Formalin-fixed paraffin embedded tissue sections from patient P's thymectomy and from normal thymic biopsies obtained anonymously from patients who underwent surgery for cardiovascular defects were stained with hematoxylin and eosin (H&E) or specific antibodies as described below in this section. Antigen was retrieved by heating slides before incubation with the primary antibody. The ChemMATE Envision Rabbit/Mouse (Dako) or Super-Sensitive Detection System (Biogenex) followed by diaminobenzidine/hydrogen peroxide, and hematoxylin counterstaining was used to visualize the signal. The following primary antibodies and reagents were used: rabbit polyclonal anti-CK5 (1:50; Covance), rat monoclonal anti-CK8 (1:200; clone TROMA-1; kindly provided by U.H. von Andrian, Harvard Medical School), rabbit polyclonal anti–claudin 4 (1:100; Zymed Laboratories), monoclonal mouse anti-Aire (1:5000; kindly provided by P. Peterson, University of Tartu), and biotin-conjugated *Ulex Europaeus* Agglutinin-1 (1:600; Vector Laboratories), all as markers of medullary thymic epithelial cell (TEC) maturation; mouse–anti-CD208/DC-LAMP (1:100; clone 104.G4; Immunotech), monoclonal mouse anti-CD11c (1:30; Novocastra Laboratories LTD), monoclonal mouse anti-CD303/BDCA2 (1:50; Dendritics), and polyclonal rabbit anti-S100 (1:5000; Dako Cytomation), as markers of dendritic cells (DCs); monoclonal rat anti-Foxp3 (1:200; eBioscience) to identify natural regulatory T cells. Images were acquired with the use of CellF imaging software (Soft Imaging System GmbH), Adobe Photoshop Version 7.0 with an Olympus DP70 camera and BX60 microscope using U plan Apochromat 10×, 20×, and 40× lenses.

Sequence analysis

Genomic DNA was extracted from peripheral blood with the use of Gentra PureGene Cell Kit. The Rag1 compound heterozygote mutations were identified by GeneDx, and the specific region was sequenced in patient and his parents with the use of primers Rag1 1304 to 1323 5′forward-CATCTTCTGTCGCTGACTCG and Rag1 (1850-1870) reverse-AAG-GTCTTGGGATCTCAT GC. Amplification was performed with 35 cycles of denaturation (95°C, 45 seconds), annealing (50°C, 30 seconds), and extension (72°C, 30 seconds), and the PCR products were cleaned with ExoSAP-IT (Amersham Pharmacia Biotech). PCR products were then sequenced on the 3100 Analyzer Sequencer with the use of the Big Dye Terminator Cycle sequencing kit (Applied Biosystems Inc) and analyzed with Seqman software (Lasergene, DNASTAR).

Determination of recombinase activity level of wild-type and mutant RAG1

Generation of retroviral vectors. pBMN-RAG1-IRES-hCD2 (CD2 allowed cell sorting as described below in "Cell culture") was constructed by inserting the *Rag1* coding region into the *Xho*I cutting site in the pBMN-IRES-hCD2 retroviral vector, which was derived from pBMN-IRES-GFP plasmid by exchanging the GFP with hCD2. The pBMN-RAG1(1566 G-T)–IRES-hCD2 and pBMN-RAG1(1621delC)–IRES-hCD2 were generated with the use of the Phusion Site-Directed Mutagenesis Kit (catalog #F-541S; NEB). The pMX-RSS-GFP/IRES-hCD4 (pMX-INV) retroviral vector has been described.[11,12]

Cell culture. Bone marrow was harvested from *Rag1*-deficient mice harboring the Eμ-Bcl-2 transgene that were generated through crossing of *Rag1*-deficient mice and the Eμ-Bcl2 transgenic mice.[13] Bone marrow cells from Rag1-/Eμ-Bcl2 transgenic mice (Y.N.L., L.W., F.W.A., unpublished data) were cultured with the pMSCV-v-abl retrovirus to generate stable v-abl transformed pro-B cell lines.[14] Pro–B-cell lines (10^6/mL) were infected with pMX-INV, from which 3 clones with single copy pMX-INV were selected and further infected with virus containing pBMN-RAG1/RAG1 (1566 G-T)/RAG1(1621delC)-IRES-hCD2.[12] Cells were treated with 3mM STI571 (Novartis), an abl kinase inhibitor, for 96 hours to promote cell differentiation.

Cells with pMX-INV and pBMN-RAG1/RAG1 (1566 G-T)/RAG1(1621delC)-IRES-hCD2 proviral integrants were isolated by magnetic bead sorting by human CD4 and human CD2 microbeads (Miltenyi Biotec GmbH) and analyzed by FACS for recombination-dependent expression of green fluorescent protein (GFP).

PBMC stimulation

PBMCs were isolated from heparinized blood with the use of standard Ficoll-Paque Premium (GE Healthcare) discontinuous gradient centrifugation. The PBMCs were washed twice with Hanks balanced salt solution without divalent cations and resuspended at 2 × 10^6/mL in RPMI containing 10% fetal calf serum (Hyclone). One hundred microliters of the cell suspension per well was cultured in a Costar no. 3596 96-well tissue flat-bottom culture plate (Corning). An equal volume of the following agonists (final concentration) was then added to separate wells: media, phytohemagglutinin (PHA; 1%; Invitrogen), lipopolysaccharide (200 ng/mL; InvivoGen), phorbol 12-myristate 13-acetate (PMA; 100 ng/mL; Sigma Chemical) plus ionomycin (1μM; Sigma Chemical), muramyl dipeptide, *Staphylococcus aureus* Cowan I (0.01%; EMD Chemicals), Pam3CSK4 (1 μg/mL), heat-killed *Listeria* monocytogenes (108 cells/mL), polyinosine-polycytidylic acid (poly I:C; 25 μg/mL), flagellin (1 μg/mL), imiquimod (1 μg/mL), single-strand RNA (ssRNA40; 10 μg/mL), and CpG DNA ODN2006 (5μM; InvivoGen). Plates were incubated in a 37°C CO_2 incubator for 48 hours. After incubation, the tissue culture plates were then spun at 300*g* for 10 minutes. The harvested supernatant was analyzed for interleukin 1β (IL-1β), IL-2, IL-6, IL-8, IL-10, IL-12p70, interferon γ, granulocyte-macrophage colony-stimulating factor, and tumor necrosis factor α (TNF-α) by multiplex cytokine analysis (Pro-Inflammatory Tissue Culture 9-Plex; MesoScale Discovery) with the use of a SECTOR Imager 6000 reader (MesoScale Discovery) per manufacturer's instructions.

Results

Patients

Subject P presented at 14 years of age after a 12-month history of loss of uvula and spontaneous tissue destruction that resulted in the erosion of his nasal septum and the extension of a pin-hole sized

A

B

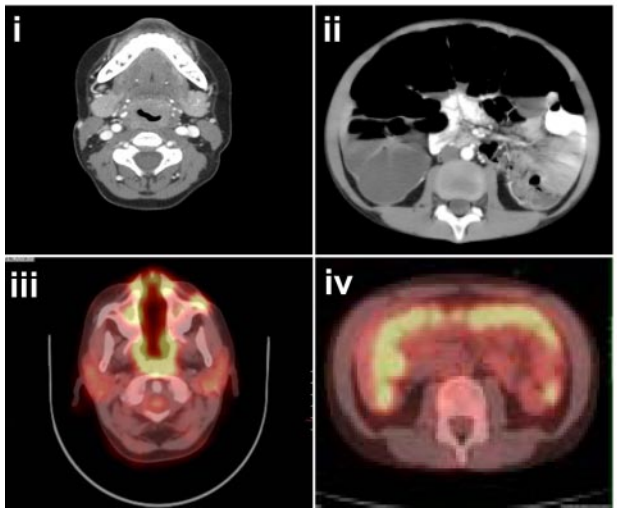

C

		14 yo			16-17 yo				19yo
	Normal range (cells/μL)	03/06 (cells/μL)	08/06 (cells/μL)	12/06 (cells/μL)	02/07 (cells/μL)	05/07 (cells/μL)	09/08 (cells/μL)	11/08 (cells/μL)	03/10 (cells/μL)
CD3 T	650-2108	1404	1180	895	914	456	129	122	664
CD4 T	362-1275	927	843	594	631	338	85	89	539
CD8 T	344-911	193	229	182	208	57	56	45	77
DNT	12-102	285	191	152	129		10	9	47
CD20	49-424	485	552	96	57		0	0	3
NK	87-505	98	89	93	140	51	97	80	153
CD4CD45RA	31-533	18	13	15	10		1	2	8
CD4CD45RO	78-520	865	790	546	572		72	71	467
CD8CD45RO	34-309						18		
CD20/CD27	16-118	343			31				2
CD3γd	9-163						17		39
CD3αβ	659-1812						112		625
IgG	642-1730mg/dL	1270						1030*	*
IgA	91-499 mg/dL	512						140*	*
IgM	34-342 mg/dL	749						479*	*
IgE	0-90 IU/mL	<5						<1.0*	*
AchR binding ab	<=0-0.02 nmol/L		1.68		0.14			0.06	*

D

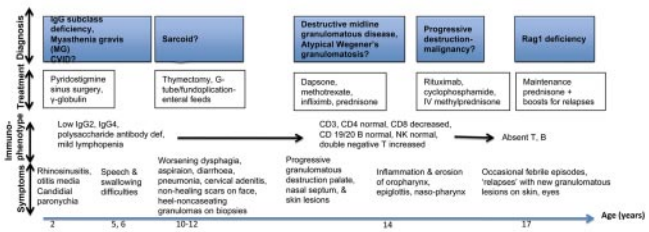

Figure 1. Granulomatous inflammation and immunophenotype on Subject P. (A) Photographs of palatal fistula at initial presentation (left), nasal fistulous tract with collapse of left alar rim (middle), and inflamed epiglottis (right). (B) Imaging studies with the use of computed tomography show the marked subglottic stenosis characteristically seen in WG (i) and megacolon (ii). Extensive inflammation in the nasopharynx (iii) and colon (iv) was evident on positron emission tomographic scans. (C) A summary of lymphocyte, immunoglobulin, and antibody levels at chronologic time points from initial diagnostic work up. *Patient on γ globulin supplement. The normal range referenced the values within 95% confidence interval, n = 40. (D) A time line depicting patient P's major clinical events chronologically (the time line is not to scale) and the progression of provisional diagnoses.

defect in his palate to a large area of his soft and hard palate (Figure 1A left), as well as appearance of skin lesions on his feet. His past history included recurrent ear and sinus infections, IgG subclass 2 and 4 deficiency, and myasthenia gravis treated with γ-globulin supplementation and pyridostigmine (a cholinesterase inhibitor), and followed by a thymectomy at 10 years of age. At presentation (14 years old), extensive workup confirmed AchR-ab positive MG; IgG2 and IgG4 deficiencies; normal frequencies of $CD3^+$ T cells, $CD19^+$ B cells, and NK cells (Figure 1C-D); mild $CD8^+$ T-cell lymphopenia; normal human leukocyte antigen I and II expression; normal antibody production to tetanus toxoid; decreased antibody production to pneumococcal polysaccharide vaccine; and notable absence of other autoantibodies especially ANCAs, anti-dsDNA, and anti-RNA. Causes of midline destructive granulomatous disease that were considered include WG, NK/T-cell lymphomas, and cocaine abuse, but circulating ANCA was negative, and molecular pathology ruled out oligoclonal lymphocytes. In the absence of evidence to confirm a diagnosis of a specific primary immune deficiency, infection, or malignancy, patient P was treated for atypical WG. He responded to the empiric treatment with methotrexate and high-dose prednisone but failed to maintain control of disease with steroid-sparing immunomodulatory drugs, including infliximab, lenalidomide, sirolimus, and mycophenolate. Further rapid progression of the disease led to the formation of a nasal fistula, nasal collapse (Figure 1A middle), and inflammation of the epiglottis (Figure 1A right), causing critical airway compromise that prompted aggressive therapy with chemotherapeutic agents, cyclophosphamide and rituximab. Control of disease was improved with high-dose steroids, and maintenance oral prednisone 40 mg/d (0.5-1 mg/kg/d) generally appeared to halt progression of disease. Over the course of his illness, a disease pattern emerged with relapses of new granulomatous lesions often occurring after febrile events, which responded to temporary boosts in prednisone dose. The immunosuppressive agents however resulted in prolonged profound T- and B-cell lymphopenia, requiring γ-globulin supplementation and antifungal and antibacterial prophylaxis. Recently, almost 3 years after the chemotherapy, a significant increase in CD3 T cells was observed, comprising almost entirely of memory CD3CD45RO memory cells, while B cells remain almost completely absent. The main medical events are summarized in Figure 1D. Given the report of granulomas in 3 girls with Rag mutations, we decided to sequence the *Rag* genes despite the unusual presentation.[14]

Subject S, an older sister of patient P, had autoimmune cytopenias and antinuclear antibody-positive collagen vascular disease that was treated with steroid pulses from age 2 to 3 years. She died at 5 years of age as a result of staphylococcal pneumonia and sepsis. Ptosis that resembled her brother's myasthenia gravis was noted months before the sepsis.

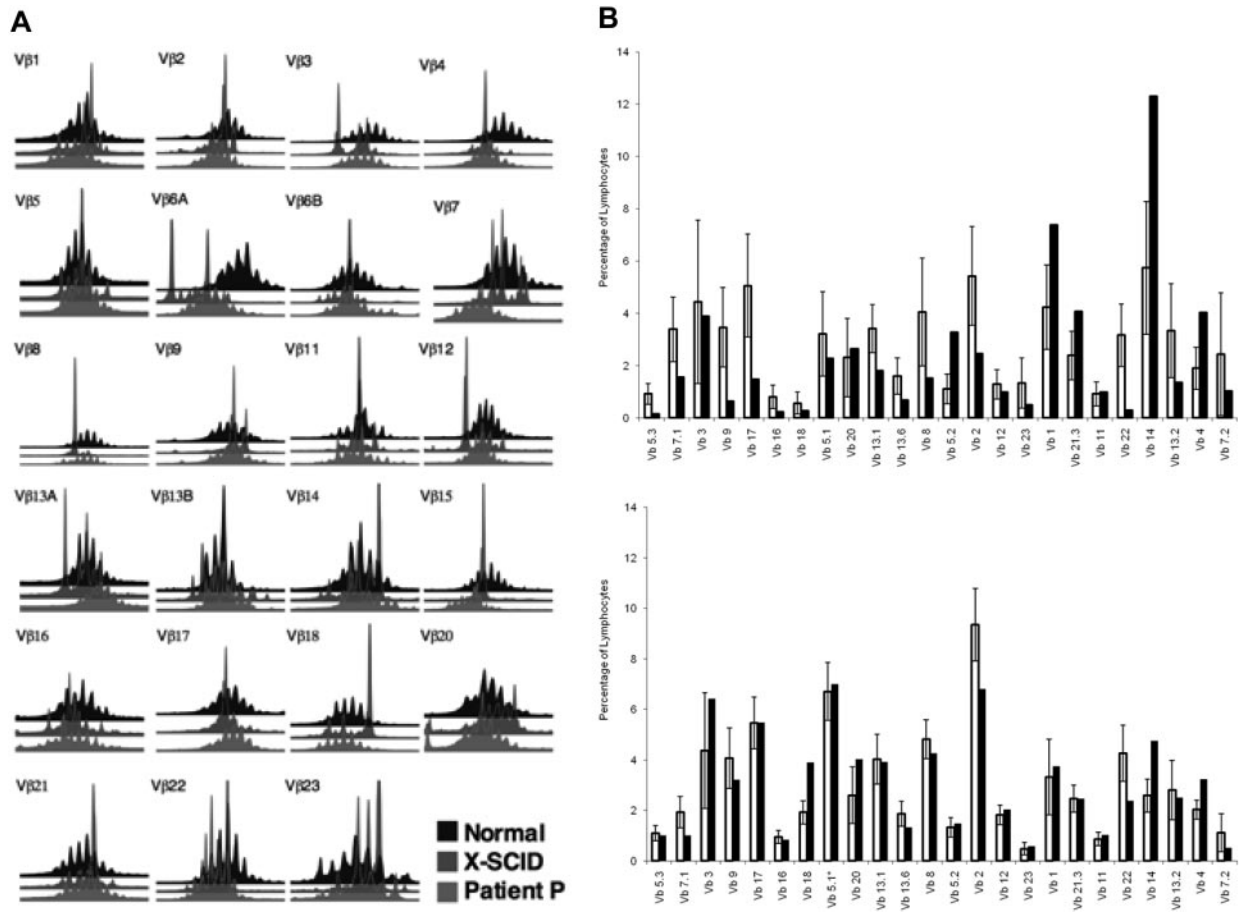

Figure 2. Diversity of T-cell receptor repertoire. (A) A diverse distribution of CDR3 lengths in most of the Vβ families was observed in the spectratype of patient P (red) compared with a healthy control (black), whereas a partially corrected γc-deficient severe combined immunodeficient patient (blue) displayed an oligoclonal repertoire. (B) Quantitative analysis of Vβ distribution in $CD4^+$ and $CD8^+$T (C) cells showed some under-presentation in a few Vβ families and over-represented in others, particularly in $CD8^+$ T cells. The shaded bars represent the patient's cells. The error bars indicate ± 1 SD.

Imaging studies

Computerized tomographic and magnetic resonance imaging studies showed extensive areas of destruction (Figure 1B); marked swelling of the proximal pharynx, including the epiglottis, creating significant subglottic stenosis characteristically seen in WG (Figure 1Bi), and distended megacolon (Figure 1Bii). A total body positron emission tomographic scan showed increased uptake at multiple sites, especially the palate (Figure 1Biii), proximal airways, and colon (Figure 1Biv), and some discrete foci on the lower legs, feet, and lungs (not shown). The areas of increased uptake on positron emission tomography correlated well with visible lesions, allowing a means to monitor disease activity.

TCR repertoire

The spectratype from patient P appeared diverse in most families and was similar to the pattern of a healthy control and was different from a representative patient with a poorly reconstituted X-linked SCID (Figure 2A). However, the repertoire evaluated by FACS with the use of monoclonal antibodies specific for individual Vβ families in $CD4^+$ (Figure 2B) and $CD8^+$ (Figure 2C) cells showed that several Vβ families are underrepresented, whereas other families appeared clonally expanded (Figure 2B-C), especially in the $CD8^+$ T cells compared with healthy controls (n = 80; Beckman Coulter). Sequencing of more than 200 of the amplified CDR3 PCR products from the patient showed similarly diverse clones as seen in a healthy volunteer.

Immunohistochemical analyses of biopsies

Multiple biopsies at various time points from many sites, including lymph node (Figure 3A), skin (Figure 3C), nasal turbinate, nasal septum, nasal tract, tongue, pharynx, cheek mass, and rectum showed acute and chronic granulomatous inflammation. In the skin, the inflammation was evident throughout the dermis and subcutaneous fat tissue with lymphohistiocytic infiltrates, epithelioid histiocytes, multinucleated giant cells, and extensive necrosis. The lymphocytic infiltrate was composed predominantly of $CD3^+$ T cells, with a preponderance of $CD8^+$ cells over $CD4^+$ cells, and no apparent $CD20^+$ B and $CD56^+$ NK cells. Multiple special stains failed to identify microorganisms at the sites of granulomatous destruction. In the biopsy of the tongue and pharynx, specific in situ hybridization for Epstein-Barr virus was negative, and, because of concerns about increased risk of malignancy, particularly a NK/T-cell lymphoma, molecular analysis for clonality of the infiltrating T cells on his tongue biopsy was performed. Because polyclonality was shown, the probability of malignancy was low.

The thymus removed from patient P at 10 years of age showed dysplastic features with fat replacement, loss of corticomedullary demarcation, and absence of Hassal corpuscles (Figure 3D). The thymic parenchyma was composed of moderate numbers of thymocytes, most of which displayed an immature blastic structure, distributed in a diffuse TEC network mainly composed of cytokeratin-5 and cytokeratin-8 double-positive immature TECs (Figure 3D).[15,16] There was an absence of autoimmune regulator (AIRE)

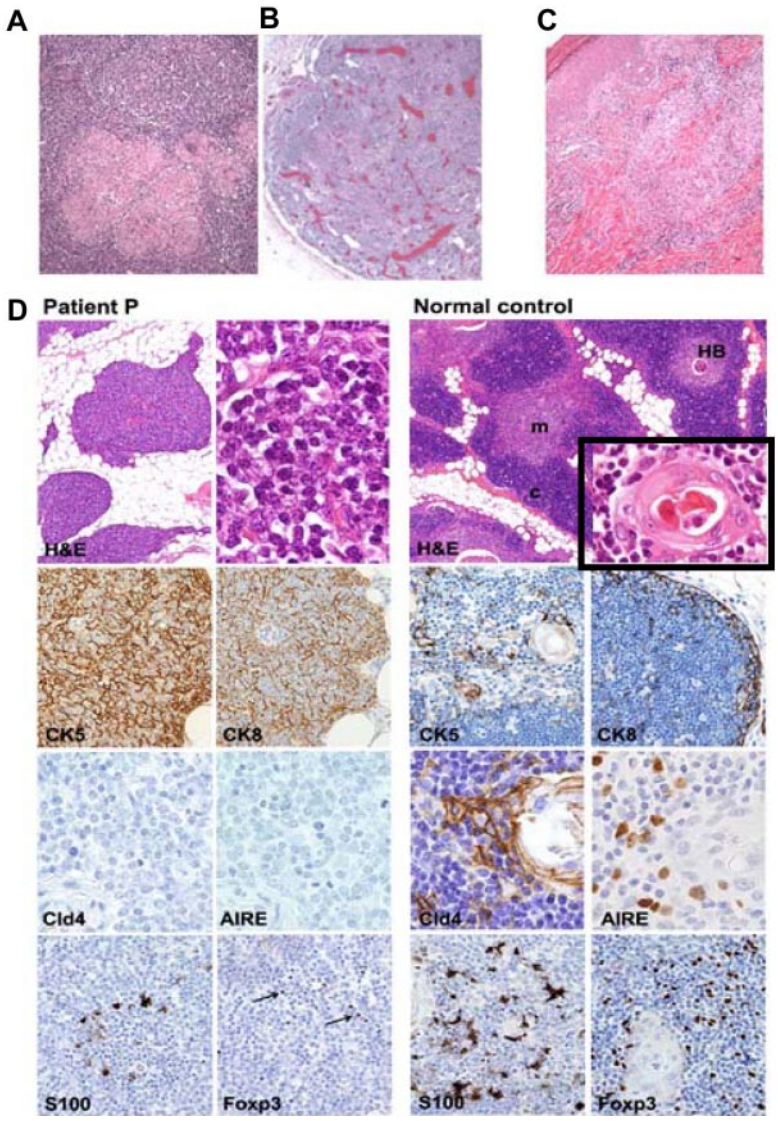

Figure 3. Immunohistopathology of lymph node, skin, and thymus. (A) Lymph node biopsy from patient P shows preserved nodal architecture with well-formed secondary B follicles and multiple epithelioid granulomas with multinucleated giant cells in the paracortical area. In contrast, lymph node at autopsy from patient's sister showed no secondary B follicles and marked polyclonal plasmacytosis (B). (C) Skin biopsy (heel) shows dense granulomatous inflammation involving mid dermis around vessels, clusters of epithelioid cells, and multinucleated giant cells. (D) Thymic biopsy shows abnormal thymic architecture with loss of corticomedullary demarcation (CMD), fat replacement and absence of Hassal bodies (HBs); moderate number of thymocytes, mostly of a blastic immature phenotype, and are admixed with TECs (top left). Immunostains highlight a diffuse epithelial network mostly composed of cytokeratin-5$^+$cytokeratin-8$^-$ (CK5$^+$CK8$^-$) double-positive immature TECs and no expression of Cld4 and AIRE (middle left). In contrast, normal thymus shows defined CMD and presence of HBs (top right and inset) with normal distribution of CK5$^+$CK8$^-$ and CK5$^-$CK8$^+$ single-positive cortical (c) and medullary (m) TECs, with expression of claudine-4 (Cld4) and AIRE (middle right). Severe depletion of thymic S-100$^+$ DCs and Foxp3$^+$ regulatory T cells (Tregs) are seen in patient (bottom left), whereas normal distribution of medullary S-100$^+$ DCs and Foxp3$^+$ Tregs were present in control thymus (bottom right; Foxp3$^+$ cells are indicated by arrows). Hematoxylin and eosin (H&E) staining, 4×, 40× (inset), and 60× original magnification; immunostains for CK5, CK8, S-100, and Foxp3, 20× magnification; immunostains for Cld4 and AIRE, 40× magnification.

and claudin-4 (CLD4), a molecule normally expressed by mature medullary TECs (Figure 3D),[17] showing a defect in TEC maturation. Immunostains for CD11c (data not shown), S-100, and Foxp3 highlighted a severe depletion of both medullary DCs and Foxp3$^+$ regulatory T cells compared with the normal thymus (Figure 3D). BDCA2, a marker of plasmacytoid DCs, was also virtually absent (data not shown).[18] The thymocytes were mostly double negative for CD4 and CD8 and lacked CD5 expression, with only a rare subset of CD8 or CD4 single-positive cells (data not shown). Histology of a lymph node showed well-formed reactive secondary B follicles and granulomas with multinucleated giant cells, compared with his sister's lymph node, which had no secondary B follicles but marked polyclonal plasmacytosis, with IgG in excess of IgA and IgM.

Rag genetic and functional analyses

Two heterozygous mutations were identified (Figure 4) in the single coding exon of the *Rag1* gene (OMIM 179615, GenBank M29474.1) (Figure 4), a G1566T missense mutation (at nucleotide 1566), resulting in a W522C replacement previously associated with atypical SCID/OS,[19] and a novel single nucleotide deletion at 1621delC, resulting in a frameshift starting with L541C to create a premature stop codon after 30 residues of a new reading frame, denoted as L541CfsX30 (Figure 4B). Sequencing of his parents identified L541CfsX30 and wild0type in his mother, whereas the missense mutation was identified in his father (Figure 4A). To measure the level of *Rag1* activity in cells expressing these mutant forms, we used an Abelson-transformed rag1-deficient pro-B cell line that contained a single integrant with an inverted GFP flanked by RSS (Figure 4C). On infection with a *Rag1*-expressing vector, exposure of the cells to STI-571, an inhibitor of abl kinase, stimulates cell differentiation and induces Rag protein expression, resulting in rearrangement and GFP detection proportional to the level of Rag activity (Figure 4D). Compared with wild-type *Rag1*, the 1621 delC mutant was completely inactive, whereas the G1566T missense mutation retained approximately 50% of normal Rag activity (Figure 4D).

Cytokine responses to stimulation

Although defective *Rag1* function could explain some of the clinical findings in this patient, a dysregulated inflammatory response was also noted. In vitro stimulation of the patient's PBMCs with a variety of stimulants was repeated several times

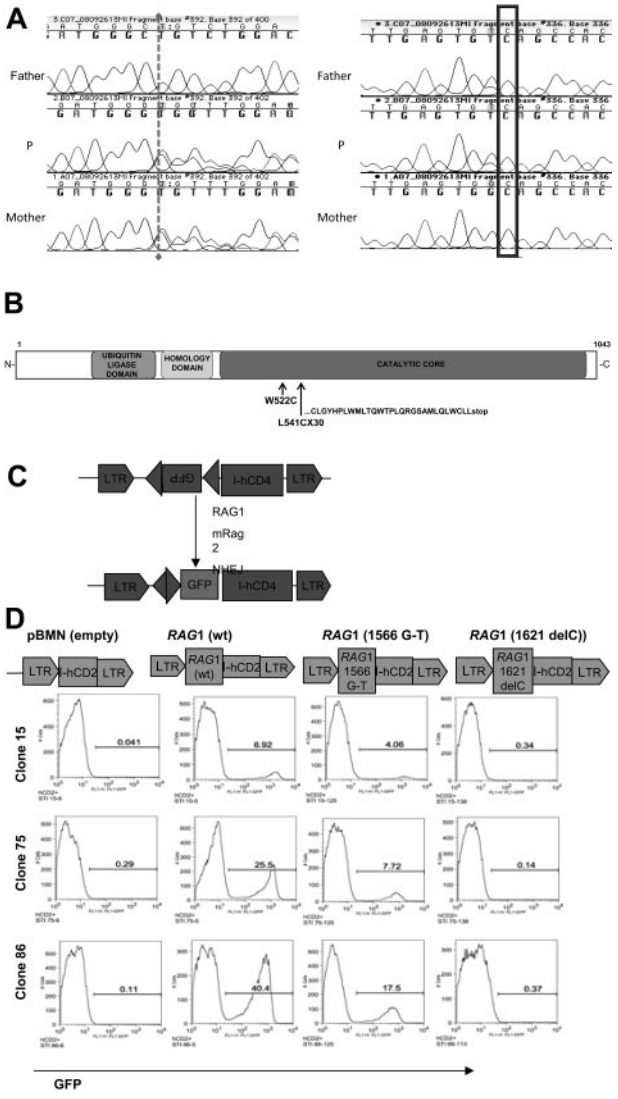

Figure 4. In vitro genetic and functional evaluation of the Rag 1 defect from Subject P. (A) Sequence analysis of the patient (middle) and his father (top) and mother (bottom), showing the novel mutation 1621delC and a previously reported 1566G > T, missense mutation (A). Both of these mutations are located within the catalytic core of RAG1 (B). (B) The effect of patient mutations on Rag1 protein. Both mutations are predicted to disrupt the catalytic domain of Rag1 with a missense W522C and the novel deletion L541CfsX30 with the resulting truncated open reading frame as indicated. (C) Mouse pro-B Abelson line deficient for Rag1 was infected with inverted substrate. (D) Subclones 1, 2, and 3 with single copy stable integrants were transduced with wild-type, G1566T, or 1621delC, then treated with STI-571 (an abl kinase inhibitor) to promote cell differentiation and induction of Rag activity. The level of GFP expression (x-axis) indicated the recombinase activity level, and only minimal GFP level was detected in the absence of STI-571.

over 3 years, and the resulting cytokine production was measured (Figure 5). For most cytokines, repeated evaluation of the responses of patient P's PBMCs did not differ significantly from the healthy controls (n = 50). In contrast, significantly elevated levels of IL-1β were observed after stimulation with PHA or poly I:C ($P < .001$ and $P = .022$, respectively; Figure 5A), but they were significantly reduced in response to other stimulants such as Pam_3CSK_4 and *L. monocytogenes* (both $P = .02$). Interestingly, IL-8 levels were also significantly elevated greater than 2- to 3-fold in response to many stimulants, in particular, PHA, phorbol 12-myristate 13-acetate, and ssRNA, as was tumor necrosis factor-α production to PHA ($P < .001$), compared with healthy controls (Figure 5B-C). Other cytokines were either not signifi-

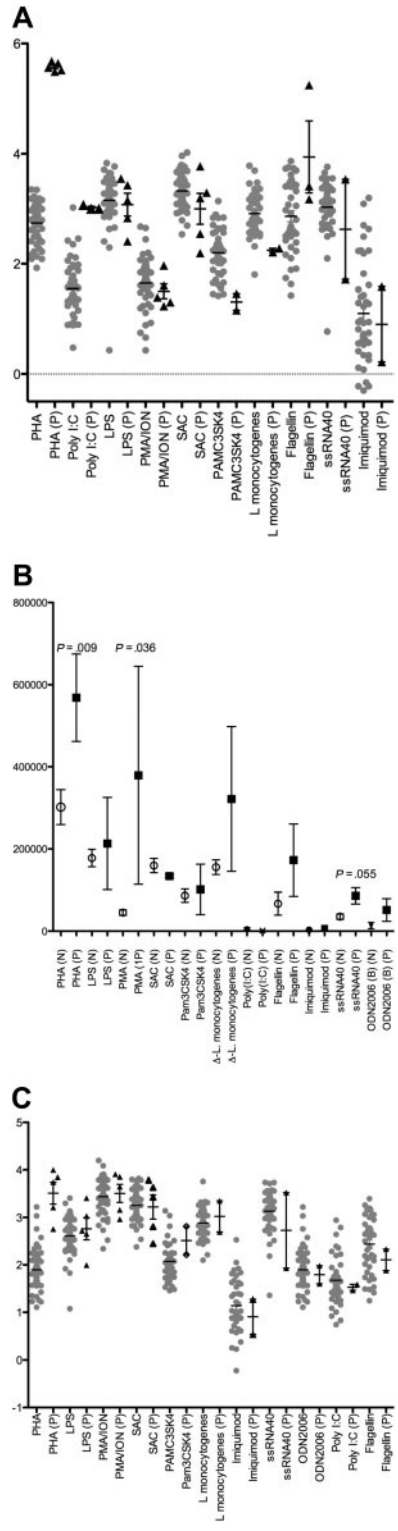

Figure 5. Stimulated cytokine responses from PBMCs. PBMCs from patient P (triangles) were challenged with indicated stimuli in vitro on multiple occasions over 3 years, and the cytokine production compared with PBMCs from healthy persons (circles) (n = 50, not age or sex matched). (A) IL-1β production was significantly increased after stimulation with pan-T cell and viral mimic (PHA and poly I:C). (B) IL-8 production in response to PHA, phorbol 12-myristate 13-acetate (PMA), or ssRNA was elevated compared with controls. (C) Production of tumor necrosis factor-α (TNFα) is also markedly elevated ($P < .001$) in response to PHA. Other cytokines measured were either not significantly different or were reduced compared with the healthy controls. LPS indicates lipopolysaccharide; ION, ionomycin; and SAC, *Staphylococcus aureus* Cowan I.

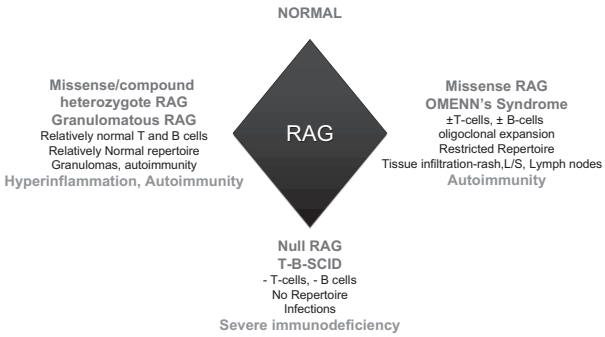

Figure 6. A model depicting key immunologic phenotypes and characteristic features in the spectrum of Rag-deficient genotypes.

cantly different or were reduced compared with the healthy controls.

Discussion

We describe a novel cause of a DMG disease as a result of hypomorphic *Rag 1* mutations. The cause of DMG based on clinical and pathology findings of progressive, necrotizing granulomas resulting in tissue destruction involving the midface, oropharynx, and upper airways include a spectrum of inflammatory and infectious diseases, of which WG and NK/T-cell lymphomas are the most common. Patient P displayed subglottic stenosis, a saddle-nose deformity, and progressive granulomatous destruction of his palate, uvula, and nasal septum typically seen in WG. The absence of clonal T or NK cells generally rules out a malignancy, although an increasing number of patients with "idiopathic midline granulomatosis" are associated with latent development of NK/T-cell malignancies. Hypomorphic mutations in many genes, including γc, *Rag1* and *Rag2*, *IL7R*, and *DNA crosslink repair-1C* (*DCLRE1C*), may result in the syndrome of SCID or OS as defined by early-onset depletion of lymphoid cells and immune deficiency resulting in susceptibility to infections. Patient P's presenting features at a relatively older age at initial assessment at 14 years of age, the normal numbers of $CD3^+$, CD19/CD20 cells, normal total IgG levels, and a relatively diverse TCR repertoire were not supportive of a SCID or OS diagnosis. The dysregulated hyperinflammation in this Rag 1-deficient phenotype expands the currently known Rag-deficient clinical spectrum (Figure 6). Granulomas have been reported in primary immunodeficiencies, including chronic granulomatous disease,[20] Blau syndrome,[14] Rag1/Rag2,[21] common variable immunodeficiency,[22,23] and Nijmegen syndrome,[24] although generally not associated with extensive tissue destruction as observed in patient P.

Both mutations disrupt catalytic domain of *Rag1*; the W522C missense mutation was previously associated with atypical SCID/OS[19] and the novel deletion at 1621delC resulting in a frameshift starting with L541C and premature truncation (denoted L541CysfsX30). These mutations were confirmed in the parents with the L541CfsX30 mutation in the mother and the W522C missense mutation in the father (Figure 4A). Because neither parent displayed obvious signs of disease, neither of these mutations is apparently dominant negative in the presence of a wild-type *Rag1* allele. Given the autoimmune cytopenias and early death of patient P's sister, she probably carried the same mutations, although her phenotype appears somewhat different. Variability in phenotypes from the same mutations in Rag even within the same family is well-recognized,[25-27] highlighting the importance of environmental factors influencing the disease manifestation.

In vitro assessment of the Rag mutants present in this patient showed recombinase activity at approximately 50% of normal with the W522C mutation and undetectable in L541CysfsX30. Up to 30% of normal Rag1 activity has been reported from some hypomorphic Rag mutations.[21] The residual recombinase activity in this patient's cells may explain his relatively mild phenotype that permits adequate recombination to generate overall normal numbers of lymphocytes, including sufficient B cells to produce normal numbers of B cells and specific antibody production. It is of interest that his IgG2 and IgG4 subclasses were deficient, and his response to polysaccharide vaccines was impaired.

Thymic dysplasia is a hallmark of primary immune deficiencies with a defect in early stages of T-cell development and often includes disruption of thymic architecture, loss of corticomedullary differentiation, absent of Hassall corpuscles, and absent DCs.[28] More recent studies of thymic disorders from a broader spectrum of patients suggested a correlation between the degree of thymic dysplasia and the severity of the T-cell defect.[18] Very early disruption of T-cell development, as seen in null mutations of γc, results in a depleted and dysplastic thymus,[28] whereas thymic structures that ranged from dysplastic and nondepleted to nearly normal were observed in hypomorphic mutations of γc or Rag1/Rag2.[18,29,30] Patient P had a nondepleted and dysplastic thymus with immature thymocytes, relatively normal numbers of circulating T and B cells, as well as total IgG level. Despite the abnormal thymic histology, he had a relatively diverse TCR repertoire, suggesting that the residual recombinase functional activity ($\leq$ 50% of normal) is probably capable of supporting a diverse repertoire. An alternate possibility is that spectratyping has a limited ability to detect subtle abnormalities in the TCR repertoire. There is a suggestion of slight skewing of a few Vβ families by flow. Sequencing of 200 individual CDR3 clones failed to detect a difference in polyclonality; however, it is possible that additional sequencing may yet show differences in his repertoire compared with normal. The lack of AIRE and $Foxp3^+$ regulatory cells (as noted in patient P's thymus) has been reported in patients with OS[31] and Rag2R229Q murine models.[32] Given AIRE's role in promoting clonal deletion of self-reactive thymocytes, dysfunctional thymic negative selection may explain the myasthenia gravis in patient P and the autoimmune cytopenias in patient S and other patients with hypomorphic Rag.[33-38] Myasthenia gravis has not been reported previously in patients with OS or those possessing other Rag mutations.

Over the course of his disease, new granulomatous lesions frequently appeared after febrile episodes that involved his skin, tongue, mucosal membranes, oro- and naso-pharynx, and eye. No infectious cause was identified, and these lesions typically improved with steroid pulses, although not always with complete resolution. The selective exaggerated responses of IL-1β and IL-8 production particularly in response to viral mimetics such as poly I:C and ssRNA and the T-lymphocyte stimulant, PHA, corresponded to the clinical pattern of relapses in patient P. Systemic viral infections such as cytomegalovirus and varicella can alter disease phenotype as can Epstein-Barr virus–associated lymphoma in Rag-deficient patients,[27,39,40] suggesting that the responses to viral antigens in hypomorphic Rag deficiency may be dysregulated; thus, environmental factors potentially play an important role as a disease modifier (Figure 6). IL-1 β is a potent inflammatory mediator, and elevated levels of IL-1β have been associated with autoinflammatory diseases[41-43] in which inflammatory destruction

of bone and cartilage is noted. In these autoinflammatory diseases, the patients may be successfully treated with anakinra, an IL-1 receptor antagonist.[42] This may be a potential agent to consider for patient P for control of future hyperinflammatory complications while considering stem cell transplantation, when an appropriate donor becomes available. The progressive destruction involving critical anatomic sites with the potential of intracranial extension in patient P led to aggressive empiric treatment, including cyclophosphamide and rituximab. This resulted in persistent profound T- and B-cell lymphopenia (now > 3 years after treatment). Rituximab is increasingly used in treating autoimmunity in patients with primary immune deficiencies to deplete potentially pathogenic B cells.[44,45] However, perhaps, depending on the underlying immune defect, long-term B-cell lymphopenia, as seen in patient P, may be a potential adverse effect to be taken into consideration before treatment.[46,47] Current standard treatment that offers potential correction for SCID is hematopoietic stem cell transplantation, although the outcome varies depending on the underlying genetic mutation, age, concurrent infections, and donor stem cell source. For patient P, nonfavorable include his previous thymectomy, the lack of a healthy matched sibling donor, and his relatively older age. The absence of a thymus will delay and may impair immune reconstitution, a problem that is further compounded if a cord blood donor is used. Hematopoietic stem cell transplantation for complete DiGeorge was reported with a combined mortality rate of greater than 40%.[48-51]

In summary, our report of a distinct Rag-deficient phenotype characterized by granulomatous inflammation and autoimmunity, with a relatively normal number of T- and B-lymphocytes and normal TCR repertoire, expands the spectrum of clinical pathology associated with Rag deficiency. In addition to defective central tolerance and peripheral regulation, our data suggest that dysregulated hyperinflammatory responses to viral antigens can lead to destructive granulomatous destruction, thus adding hyperinflammation to the current known Rag-deficiency features of infection and autoimmunity (Figure 6).

Acknowledgments

This work was supported by the NIAID Division of Intramural Research and the Clinical Center of the NIH. It was also funded in part by the National Cancer Institute, National Institutes of Health (contract N01-CO-12400).

The content of this publication does not necessarily reflect the views or policies of the Department of Health and Human Services, nor does mention of trade names, commercial products, or organizations imply endorsement by the US government.

The publisher or recipient acknowledges right of the US government to retain a nonexclusive, royalty-free license in and to any copyright covering the article.

Authorship

Contribution: S.S.D.R. designed and performed experiments and wrote the paper; E.W.C., D.B.K., K.A.Z., N.L.T.-W., J.E.N., Y.N.L., L.W., F.W.A., P.L.P., and N.G.S. performed experiments, analyzed results, and made figures; K.A.Z., E.M.K., J.D.M., D.C.D., S.P., S.H.S., M.F.-P., an H.L.M. analyzed results and edited the paper.

Conflict-of-interest disclosure: The authors declare no competing financial interests.

Correspondence: Suk See De Ravin, Laboratory of Host Defenses, National Institutes of Allergy and Infectious Diseases, NIH, CRC-5W Rm 5-3816, 10 Center Dr, Bethesda, MD 20892; e-mail: sderavin@niaid.nih.gov.

References

1. Rodrigo JP, Suarez C, Rinaldo A, et al. Idiopathic midline destructive disease: fact or fiction. *Oral Oncol.* 2005;41(4):340-348.
2. Sheahan P, Donnelly M, O'Reilly S, Murphy M. T/NK cell non-Hodgkin's lymphoma of the sinonasal tract. *J Laryngol Otol.* 2001;115(12):1032-1035.
3. Devaney KO, Travis WD, Hoffman G, Leavitt R, Lebovics R, Fauci AS. Interpretation of head and neck biopsies in Wegener's granulomatosis. A pathologic study of 126 biopsies in 70 patients. *Am J Surg Pathol.* 1990;14(6):555-564.
4. Hesslein DG, Schatz DG. Factors and forces controlling V(D)J recombination. *Adv Immunol.* 2001;78:169-232.
5. Bassing CH, Chua KF, Sekiguchi J, et al. Increased ionizing radiation sensitivity and genomic instability in the absence of histone H2AX. *Proc Natl Acad Sci U S A.* 2002;99(12):8173-8178.
6. Gellert M. V(D)J recombination: RAG proteins, repair factors, and regulation. *Annu Rev Biochem.* 2002;71:101-132.
7. Roth DB. Restraining the V(D)J recombinase. *Nat Rev Immunol.* 2003;3(8):656-666.
8. Landay AL, Muirhead KA. Procedural guidelines for performing immunophenotyping by flow cytometry. *Clin Immunol Immunopathol.* 1989;52(1):48-60.
9. Bousso P, Wahn V, Douagi I, et al. Diversity, functionality, and stability of the T cell repertoire derived in vivo from a single human T cell precursor. *Proc Natl Acad Sci U S A.* 2000;97(1):274-278.
10. Pannetier C. *The Antigen T Cell Receptor: Selected Protocols and Applications.* Austin, TX: Landes; 1997.
11. Liang HE, Hsu LY, Cado D, Cowell LG, Kelsoe G, Schlissel MS. The "dispensable" portion of RAG2 is necessary for efficient V-to-DJ rearrangement during B and T cell development. *Immunity.* 2002;17(5):639-651.
12. Bredemeyer AL, Sharma GG, Huang CY, et al. ATM stabilizes DNA double-strand-break complexes during V(D)J recombination. *Nature.* 2006;442(7101):466-470.
13. Strasser A, Whittingham S, Vaux DL, et al. Enforced BCL2 expression in B-lymphoid cells prolongs antibody responses and elicits autoimmune disease. *Proc Natl Acad Sci U S A.* 1991;88(19):8661-8665.
14. Mainville CA, Parmar K, Unnikrishnan I, Gong L, Raffel GD, Rosenberg N. Temperature-sensitive transformation by an Abelson virus mutant encoding an altered SH2 domain. *J Virol.* 2001;75(4):1816-1823.
15. Gill J, Malin M, Sutherland J, Gray D, Hollander G, Boyd R. Thymic generation and regeneration. *Immunol Rev.* 2003;195:28-50.
16. Hollander G, Gill J, Zuklys S, Iwanami N, Liu C, Takahama Y. Cellular and molecular events during early thymus development. *Immunol Rev.* 2006;209:28-46.
17. Hollander GA. Claudins provide a breath of fresh Aire. *Nat Immunol.* 2007;8(3):234-236.
18. Poliani PL, Facchetti F, Ravanini M, et al. Early defects in human T-cell development severely affect distribution and maturation of thymic stromal cells: possible implications for the pathophysiology of Omenn syndrome. *Blood.* 2009;114(1):105-108.
19. Villa A, Sobacchi C, Notarangelo LD, et al. V(D)J recombination defects in lymphocytes due to RAG mutations: severe immunodeficiency with a spectrum of clinical presentations. *Blood.* 2001;97(1):81-88.
20. Segal BH, Leto TL, Gallin JI, Malech HL, Holland SM. Genetic, biochemical, and clinical features of chronic granulomatous disease. *Medicine (Baltimore).* 2000;79(3):170-200.
21. Schaffer JV, Chandra P, Keegan BR, Heller P, Shin HT. Widespread granulomatous dermatitis of infancy: an early sign of Blau syndrome. *Arch Dermatol.* 2007;143(3):386-391.
22. Schuetz C, Huck K, Gudowius S, et al. An immunodeficiency disease with RAG mutations and granulomas. *N Engl J Med.* 2008;358(19):2030-2038.
23. Pujol RM, Nadal C, Taberner R, Diaz C, Miralles J, Alomar A. Cutaneous granulomatous lesions in common variable immunodeficiency: complete resolution after intravenous immunoglobulins. *Dermatology.* 1999;198(2):156-158.
24. Torrelo A, Mediero IG, Zambrano A. Caseating cutaneous granulomas in a child with common variable immunodeficiency. *Pediatr Dermatol.* 1995;12(2):170-173.
25. Yoo J, Wolgamot G, Torgerson TR, Sidbury R. Cutaneous noncaseating granulomas associated with Nijmegen breakage syndrome. *Arch Dermatol.* 2008;144(3):418-419.

26. Le Deist F, de Villartay JP, Lim A, Dechanet J, Fischer A. [Hypomorphic RAG1 mutations and CMV infection: a new phenotype of severe combined immunodeficiency]. *Med Sci (Paris).* 2006; 22(3):239-240.
27. Jaouad IC, Ouldim K, Ali Ou Alla S, Kriouile Y, Villa A, Sefiani A. Omenn syndrome with mutation in RAG1 gene. *Indian J Pediatr.* 2008;75(9):944-946.
28. Karaca NE, Aksu G, Genel F, et al. Diverse phenotypic and genotypic presentation of RAG1 mutations in two cases with SCID. *Clin Exp Med.* Prepublished on May 21, 2009, as DOI 10.1007/s10238-009-0053-1. (Now available as *Clin Exp Med.* 2009;9(4):339-342).
29. Hale LP, Buckley RH, Puck JM, Patel DD. Abnormal development of thymic dendritic and epithelial cells in human X-linked severe combined immunodeficiency. *Clin Immunol.* 2004;110(1):63-70.
30. Sharfe N, Shahar M, Roifman CM. An interleukin-2 receptor gamma chain mutation with normal thymus morphology. *J Clin Invest.* 1997;100(12):3036-3043.
31. Poliani PL, Vermi W, Facchetti F. Thymus microenvironment in human primary immunodeficiency diseases. *Curr Opin Allergy Clin Immunol.* 2009; 9(6):489-495.
32. Cavadini P, Vermi W, Facchetti F, et al. AIRE deficiency in thymus of 2 patients with Omenn syndrome. *J Clin Invest.* 2005;115(3):728-732.
33. Marrella V, Poliani PL, Casati A, et al. A hypomorphic R229Q Rag2 mouse mutant recapitulates human Omenn syndrome. *J Clin Invest.* 2007; 117(5):1260-1269.
34. Liston A, Lesage S, Wilson J, Peltonen L, Goodnow CC. Aire regulates negative selection of organ-specific T cells. *Nat Immunol.* 2003;4(4): 350-354.
35. Milner JD, Fasth A, Etzioni A. Autoimmunity in severe combined immunodeficiency (SCID): lessons from patients and experimental models. *J Clin Immunol.* 2008;28 Suppl 1:S29-33.
36. Somech R, Simon AJ, Lev A, et al. Reduced central tolerance in Omenn syndrome leads to immature self-reactive oligoclonal T cells. *J Allergy Clin Immunol.* 2009;124(4):793-800.
37. Anderson MS, Venanzi ES, Chen Z, Berzins SP, Benoist C, Mathis D. The cellular mechanism of Aire control of T cell tolerance. *Immunity.* 2005; 23(2):227-239.
38. Hubert FX, Kinkel SA, Webster KE, et al. A specific anti-Aire antibody reveals aire expression is restricted to medullary thymic epithelial cells and not expressed in periphery. *J Immunol.* 2008; 180(6):3824-3832.
39. Kyewski B, Klein L. A central role for central tolerance. *Annu Rev Immunol.* 2006;24:571-606.
40. de Villartay JP, Lim A, Al-Mousa H, et al. A novel immunodeficiency associated with hypomorphic RAG1 mutations and CMV infection. *J Clin Invest.* 2005;115(11):3291-3299.
41. Dalal I, Tabori U, Bielorai B, et al. Evolution of a T-B- SCID into an Omenn syndrome phenotype following parainfluenza 3 virus infection. *Clin Immunol.* 2005;115(1):70-73.
42. Aksentijevich I, Nowak M, Mallah M, et al. De novo CIAS1 mutations, cytokine activation, and evidence for genetic heterogeneity in patients with neonatal-onset multisystem inflammatory disease (NOMID): a new member of the expanding family of pyrin-associated autoinflammatory diseases. *Arthritis Rheum.* 2002;46(12):3340-3348.
43. Aksentijevich I, Masters SL, Ferguson PJ, et al. An autoinflammatory disease with deficiency of the interleukin-1-receptor antagonist. *N Engl J Med.* 2009;360(23):2426-2437.
44. Reddy S, Jia S, Geoffrey R, et al. An autoinflammatory disease due to homozygous deletion of the IL1RN locus. *N Engl J Med.* 2009;360(23): 2438-2444.
45. Guzman Moreno R. B-cell depletion in autoimmune diseases. Advances in autoimmunity. *Autoimmun Rev.* 2009;8(7):585-590.
46. Lafyatis R, Kissin E, York M, et al. B cell depletion with rituximab in patients with diffuse cutaneous systemic sclerosis. *Arthritis Rheum.* 2009;60(2): 578-583.
47. Rao A, Kelly M, Musselman M, et al. Safety, efficacy, and immune reconstitution after rituximab therapy in pediatric patients with chronic or refractory hematologic autoimmune cytopenias. *Pediatr Blood Cancer.* 2008;50(4):822-825.
48. Rao VK, Price S, Perkins K, et al. Use of rituximab for refractory cytopenias associated with autoimmune lymphoproliferative syndrome (ALPS). *Pediatr Blood Cancer.* 2009;52(7):847-852.
49. Land MH, Garcia-Lloret MI, Borzy MS, et al. Long-term results of bone marrow transplantation in complete DiGeorge syndrome. *J Allergy Clin Immunol.* 2007;120(4):908-915.
50. Bowers DC, Lederman HM, Sicherer SH, Winkelstein JA, Chen AR. Immune constitution of complete DiGeorge anomaly by transplantation of unmobilised blood mononuclear cells. *Lancet.* 1998;352(9145):1983-1984.
51. Markert ML. Treatment of infants with complete DiGeorge anomaly [letter]. *J Allergy Clin Immunol.* 2008;121(4):1063, author reply 1063-1064.